

Experimental Demonstration of Wavelength-Selective Band/Direction-Switchable Multi-Band OXC Using an Inter-Band All-Optical Wavelength Converter

Hiroki Kawahara⁽¹⁾, Masahiro Nakagawa⁽¹⁾, Takeshi Seki⁽¹⁾ and Takashi Miyamura⁽¹⁾

⁽¹⁾ NTT Network Service System Laboratories, hiroki.kawahara.vp@hco.ntt.co.jp

Abstract We propose a highly-flexible multi-band OXC which effectively utilizes enhanced network resources through multi-band WDM for the first time. We experimentally confirm the feasibility of the newly-proposed C+L-band OXC with wavelength-selective band/direction switching functions.

Introduction

In recent years, spectrum parallelism based on multi-band wavelength-division multiplexing (MB-WDM) transmission technology has been extensively studied to cost-effectively expand capacity^[1-3]. Other than C band, this approach utilizes unused bands such as O, E, S, L on already-deployed standard single-mode fiber. However, the impact of inter-band stimulated Raman scattering (ISRS) should be considered in MB-WDM system design since power transition from shorter to longer wavelengths causes strong transmission-band dependency on the signal-to-noise ratio (SNR), which becomes serious as more bands are used^[4]. For MB network systems, lightpath provisioning is mostly blocked by insufficient optical reach especially on the severely SNR-degraded bands in addition to the wavelength-continuity constraints. Thus, spectral utilization is severely restricted despite the capacity extension^{[5],[6]}. To overcome this problem, we have introduced path assignment of individual wavelength channels to arbitrary bands and directions onto MB networks to relax not only wavelength-continuity but also ISRS-induced optical-reach constraints can be relaxed^[7]. However, multi-band optical cross-connect (MB-OXC) such highly-flexible switching functions has not yet been proposed.

In this paper, we propose a relatively practical MB-OXC that enables wavelength-selective switching of bands and directions using an inter-band all-optical wavelength converter and explain its benefits. Next, we report experimental results about the feasibility of newly-proposed C+L-band OXC supporting 112-Gbit/s dual polarization quadrature phase-shift keying (DP-QPSK) signal transmission.

Proposed multi-band OXC

Figure 1 (a) shows a conventional MB-OXC configuration supporting O, E, S, C and L bands, which consists of a multi-band multiplexer and

demultiplexer (MB-MUX/DEMUX), and multi-band wavelength cross-connect (MB-WXC). MB-WXC was configured by deploying multiple single-band WXCs (SB-WXCs) in parallel where ingress and egress wavelength-selective switches (WSSs) are independently connected with full mesh for each band. For such WXC configurations, individual wavelength channels can be switched to any direction within each band but cannot be switched to any band even though such a degree of freedom is necessary to effectively utilize enhanced network resources through MB-WDM.

On the contrary, Figure 1 (b) shows our proposed MB-OXC with wavelength-selective switching to any bands and directions, which consists of MB-MUX/DEMUX units and an ingress and egress inter-band all-optical wavelength converter (AO-WC) to convert multiple wavelengths to and from C band, and a C-band WXC in which all ingress and egress C-band WSSs are connected with full mesh. For this configuration, individual wavelength channels within each band can be freely switched to any bands and directions.

A key component of the proposed MB-OXC is inter-band AO-WC, which allows wideband and multiple-wavelength conversion and modulation-formant/bitrate agnostic operation unlike field-deployed O/E/O-based WC. Note that according to recent progressive studies^{[8],[9]}, a compact and practical device for AO-WC based on periodically poled LiNbO₃ waveguides or highly-nonlinear fiber can be deployed.

Benefits of the proposed multi-band OXC

The proposed MB-OXC has several benefits, as listed below.

(i) Individual wavelength channels can be freely switched to any band and direction.

1. Effective utilization of network resources by relaxing ISRS-induced optical-reach and wavelength-continuity constraints.
2. Transparent handover on heterogeneous MB networks utilizing different bands.

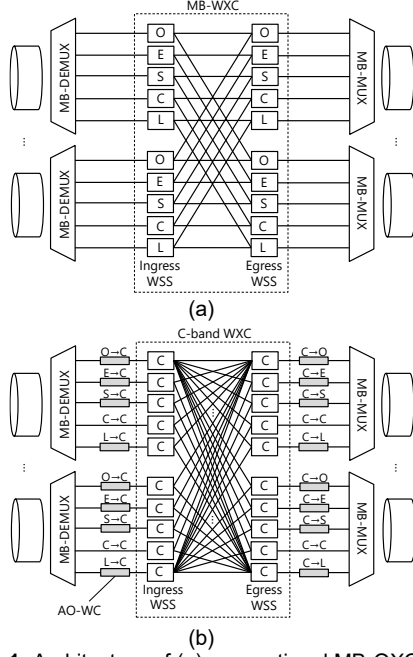


Fig. 1: Architecture of (a) conventional MB-OXC and (b) proposed MB-OXC.

3. Suitable band selection for different fiber types to improve optical performance.
- (ii) WXC function can be implemented only with commonly available C-band WSS.
1. Exclusion of low-maturity WDM components such as O-, E-, S-band WSSs^[10]; This can prevent market fragmentation which improves market availability and lowers increase of operational complexity of the network.
 2. Adoption of previously-proposed small-scale single-band WXC architecture^{[11], [12]}.
 3. Compact implementation of WXC function by single-band multiple-arrayed WSS technique^{[13], [14]}.

As follows, we explain the benefit (i)-1, as reported in the numerical analysis of the benefits in [7]. Here, we describe how wavelength-selective band switching capability can mitigate the impact of ISRS. We considered a 15-THz S-, C-, and L-band 50-GHz-spaced 300-channel WDM system. Each WDM channel is Gaussian-modulated and transmitted over 10 100-km spans of single-mode fiber (SMF) where the attenuation, dispersion, dispersion slopes, and nonlinear coefficient, and Raman gain slopes are 0.2 dB/km, 17 ps/nm/km, 0.067 ps/nm²/km, 1.2 1/W/km, and 0.028 1/W/km/THz, respectively. The fiber launch power per channel is -2 dBm. At the end of each span, the span loss and the SRS-induced tilt were compensated by erbium-doped fiber amplifier (EDFA) and thulium-doped fiber amplifier (TDFA) with noise figures of 7, 5, and 6 dB in the S, C and L band, respectively. For such systems, a generalized SNR (GSNR) after 1 span was calculated using a closed form based

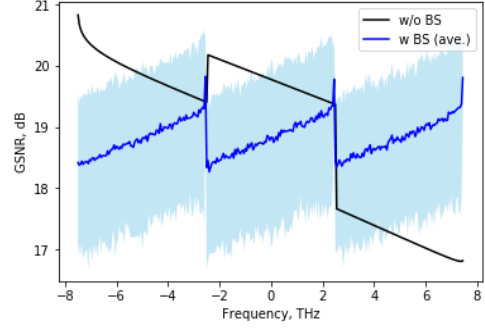


Fig. 2: Statistical distribution of GSNR after 10 spans without and with band-switching.

on ISRS GN model^[15]. Then, without a band switching, GSNR after 10 spans was calculated by adding up incoherently nonlinear interference (NLI) and ASE noise generated by each fiber span. With the band switching, band of each channel was assumed to be switched randomly and uniformly span by span. Considering such random effects, we employed Monte-Carlo simulations to evaluate the statistical distribution of the GSNR after 10 spans of 1000 different band-switching scenarios. The results of these simulations are shown in Fig. 2, where the black line indicates the deterministic GSNR without the band switching, and the blue line and shaded area show the averaged value and 3- σ ranges of the GSNR with band switching. As expected, in high-frequency bands with severely degraded SNR, the GSNR significantly improves by averaging out the impact of ISRS due to the band switching.

Experimental setup and results

Figure 3 (a) shows the setup for the transmission experiment, which represents a 2-degree C- and L-band proposed MB-OXC. The configuration of proposed MB-OXC is similar to the one shown in Fig. 1(b) where C- and L-band EDFA pre- and post-amplifiers were added to each input and output directional port. Each ring consisted of a 60-km single-mode fiber (SMF) and a C-band backward distributed Raman amplifier (DRA) that compensates a spectral tilt due to ISRS. Inter-band AO-WC was based on four-wave mixing (FWM) over a highly-nonlinear fiber and implemented in a similar manner to that in [8]. Egress WSS equalized the wavelength-dependent gain the AO-WC and EDFA. 50-GHz-spaced 72-channel (from 1529.55 to 1556.96 nm) 112-Gbit/s dual polarization quadrature phase shift keying (DP-QPSK) signals were generated and one of them was replaced with the 112-Gbit/s DP-QPSK signal output from a real-time transponder. The C-band WDM signal was added to OXC and launched on the ring 1 route. After the first span transmission, the proposed MB-OXC delivered individual wavelength channels to ring 1 or 2 by

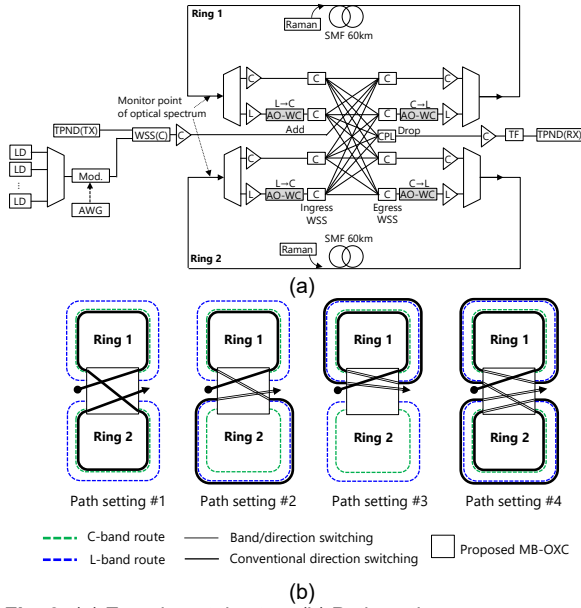


Fig. 3: (a) Experimental setup. (b) Path setting patterns to verify the band-switching capability.

the direction-switching function, and to C- and L-band routes by the band-switching function. The channel launch power is 3 dBm/ch at rings 1 and 2. Figure 3 (b) shows the path setting patterns to verify the wavelength-selective band/direction switching function where the green and blue dotted line indicate the C- and L-band routes, and the black solid line shows the paths corresponding to the path setting pattern #1~#4 that are assigned to every 4 channels of the 72-channel WDM signal. The C- and L-band WDM signal spectra in each ring was monitored at the end of the ring to confirm the wavelength-selective band/direction switching function. Through optical coupler for drop, EDFA and tunable filter (TF), individual channel within C-band WDM signal was incident into the receiver, and Q-factor was measured in real-time.

Figure 4 (a) shows overall optical spectra and expanded spectra of a section monitored at the end of ring 1 and 2, which represents the wavelength-selective band/direction switching capability provided by the proposed MB-OXC. For instance, the wavelength channel assigned for path setting #4 was transmitted in C-band ring 1 route for the first span, L-band ring 1 route for second span, C-band ring 1 route for third span, and L-band ring 2 route for fourth span, respectively.

Figure 5 (a) and (b) shows Q factors and penalties, respectively. The Q penalties were calculated by subtracting the measured Q factors with the Q factors estimated from the measured OSNR, based on pre-measured back-to-back Q-over-OSNR characteristics. Q factors of all 72 channels greatly exceed the Q limit of 5.2 dB. However, there were moderate penalties of < 0.5 dB, < 1.4 dB, < 1.4 dB, and < 2.4 dB for

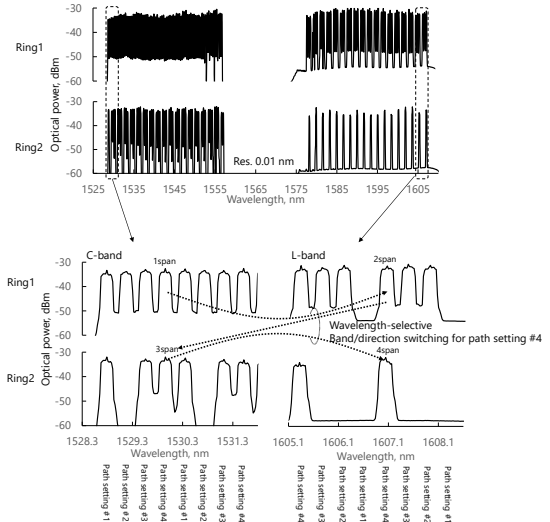


Fig. 4: Optical signal spectrum at the end of ring 1 and 2

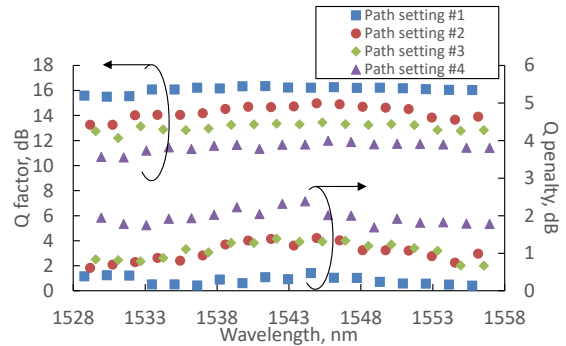


Fig. 5: Q factors and penalties

path settings #1 ~ #4, respectively. The Q penalty for the path setting #2 significantly increased compared to #1, as did that for #3 compared to #4. There were two factors for significant penalties. One was that the penalty predominantly came from the nonlinearity inside the AO-WC operating in the multiple wavelength condition by passing through one pair of C-to-L and L-to-C AO-WC. We believe that such penalty can be suppressed by finely tuning the FWM generation condition of AO-WC. The other was that a strong Kerr effect by ISRS-induced power transfer imposed the deterioration on L-band WDM signal though SMF transmission due to insufficient optimization of fiber launch power for each ring.

Conclusions

We described a wavelength-selective band/direction-switchable multi-band OXC using an inter-band all-optical wavelength converter, for the first time. We demonstrated experimentally a feasibility of the newly-proposed C+L-band OXC supporting 112-Gbit/s DP-QPSK signal transmission.

References

- [1] F. Hamaoka, M. Nakamura, S. Okamoto, K. Minoguchi, T. Sasai, A. Matsushita, E. Yamazaki, and Y. Kisaka, "Ultra-wideband WDM transmission in S-, C-, and L-bands using signal power optimization scheme," *IEEE J. of Lightw. Technol.*, vol. 38, no. 8, Apr. 2019.
- [2] J. Renaudier, A. Carbo Meseguer, A. Ghazisaeidi, P. Tran, R. Rios Muller, R. Brenot, A. Verdier, F. Blache, K. Mekhazni, B. Duval, H. Debregeas, M. Achouche, A. Boutin, F. Morin, L. Letteron, N. Fontaine, Y. Frignac, and G. Charlet, "First 100-nm continuous-band WDM transmission system with 115 Tb/s transport over 100km using novel ultra-wideband semiconductor optical amplifiers," in *Proc. Eur. Conf. Opt. Commun.*, Gothenburg, Sweden, Sep. 2017, Paper Th.PDP.A.3.
- [3] M. A. Iqbal, L. Krzczanowicz, I. Phillips, P. Harper, and W. Fprysiak, "150nm SCL-band transmission through 70km SMF using ultra-sideband dual-stage discrete Raman amplifier," in *Proc. Opt. Fiber Commun. Conf.*, San Diego, CA, USA, Mar. 2020, Paper W3E.4.
- [4] S. Okamoto, K. Minoguchi, F. Hamaoka, K. Horikoshi, A. Matsushita, M. Nakamura, E. Yamazaki, and Y. Kisaka, "A study on the effect of ultra-wide band WDM on optical transmission systems," *IEEE J. of Lightw. Technol.*, vol. 38, no. 5, Mar. 2020.
- [5] H. Zang, J. P. Jue, and B. Mukherjee, "A review of routing and wavelength assignment approaches for wavelength-routed optical WDM networks," *Opt. Netw. Mag.*, vol. 1, no. 1, Jan. 2000.
- [6] N. Sambo, A. Ferrari, A. Napoli, N. Costa, J. Pedro, B. Sommerkorn-Krombholz, P. Castoldi, and V. Curri, "Provisioning in Multi-band optical networks," *IEEE J. of Lightw. Technol.*, vol. 38, no. 9, May. 2020.
- [7] M. Nakagawa, H. Kawahara, T. Seki, T. Matsuda, and T. Miyamura, "Benefits of Wavelength-Selective Band Switching Capability on Multi-Band Optical Networks," *Proc. Eur. Conf. Opt. Commun.*, Brussels, Belgium, Dec. 2020, to be published.
- [8] T. Kato, S. Watanabe, T. Yamauchi, G. Nakagawa, H. Muranaka, Y. Tanaka, Y. Akiyama, and T. Hoshida, "Real-time transmission of 240x200-Gb/s signal in S+C+L triple-band WDM without S- or L-band transceivers," in *Proc. Eur. Conf. Opt. Commun.*, Dublin, Ireland, Sep. 2019, Paper PD.1.7.
- [9] C. Wang, C. Langrock, A. Marandi, M. Jankowski, M. Zhang, B. Desiatov, M. M. Fijer, and M. Loncar, "Ultrahigh-efficiency wavelength conversion in nanophotonic periodically poled lithium niobite waveguides," *OSA Optica*, vol. 5, no.11, Nov. 2018.
- [10] A. Ferrari, A. Napoli, J. K. Fischer, N. Costa, A. D'Amico, J. Pedro, W. Forysiak, E. Pincemin, A. Lord, A. Stavdas, J. Pedro, F. -P. Gimenez, G. Roelkens, N. Calabretta, S. Abrate, B. Sommerkorn-Krombholz, and V. Curri, "Assessment on the achievable throughput of multi-band ITU-T G.652.D fiber transmission systems," *IEEE J. of Lightw. Technol.*, vol. 38, no. 16, Apr. 2020.
- [11] Y. Iwai, H. Hasegawa, and K. Sato, "A large-scale photonic node architecture that utilizes interconnected OXC subsystems," *OSA Opt. Exp.*, vol. 21, no. 1, Jan. 2013.
- [12] A. Sahara, H. Kawahara, S. Yamamoto, S. Kawai, M. Fukutoku, T. Mizuno, Y. Miyamoto, K. Suzuki, and K. Yamaguchi, "Proposal and experimental demonstration of SDM node enabling path assignment to arbitrary wavelengths, cores, and directions," *OSA. Opt. Exp.*, vol. 25, no.4, Feb. 2017.
- [13] H. Kawahara, A. Sahara, Y. Sone, S. Kawai, M. Fukutoku, Y. Miyamoto, K. Yamaguchi, K. Suzuki, and T. Hashimoto, "First investigation and reduction of inter-WSS crosstalk in multiple-arrayed WSSs for large-scale optical node," in *Proc. CLEO-PR/OECC/PGC2017*, Paper 3-2K-2.
- [14] K. Yamaguchi, K. Seno, K. Suzuki, H. Kawahara, M. Fukutoku, T. Hashimoto, and Y. Miyamoto, "Integrated wavelength selective switch array for space division multiplexed network with ultra-low inter-spatial channel crosstalk," in *Proc. Opt. Fiber Commun. Conf.*, San Francisco, CA, USA, Mar. 2018, Paper Th1J.3.
- [15] D. Semaru, R. I. Killey, and P. Bayvel, "A closed-form approximation of the Gaussian noise model in the presence of inter-channel stimulated Raman scattering," *IEEE J. of Lightw. Technol.*, vol. 37, no. 9, May. 2019.